



Full factorial experimental design analysis of Rhodamine B removal from water using organozeolite from coal bottom ash

Raquel R. Alcântara, Rafael O. R. Muniz, Denise A. Fungaro

Chemical and Environmental Center, Nuclear and Energy Research Institute, Sao Paulo, Brazil.

Abstract

Zeolitic material synthesized using coal bottom ash as raw material was modified by cationic surfactant. Raw bottom ash and zeolitic materials were characterized using various techniques to obtain its physical and chemical properties. Surfactant modified zeolite (SMZBA) was used as alternative low-cost adsorbent for removal of Rhodamine B (RB) dye from aqueous solution. Dye adsorption equilibrium was attained after 40 min of the contact time and adsorption kinetics were described by the pseudo second order kinetic model. Equilibrium adsorption data were adjusted using non-linear equations of the Langmuir, Freundlich, Temkin and Dubinin-Radushkevich (D-R) models. Error analysis showed that D-R was the most appropriate for fitting the experimental data. The reuse of the remaining solution generated from the synthesis of zeolite was effective. To optimize the operating conditions, the temperature, pH, adsorbent dosage and initial concentration of the dye were investigated by full factorial experimental design method; adsorbent dosage, initial concentration and interaction of the two were found as the most significant factors with $P = 0.02$ lower than 95% confidence level. The results showed that SMZBA is a good adsorbent for the removal of RB from aqueous effluent.

Copyright © 2016 International Energy and Environment Foundation - All rights reserved.

Keywords: Surfactant-modified zeolite; Bottom ash, Rhodamine B; Remaining solution; Factorial experimental design.

1. Introduction

Brazil is one of the largest and more important Gem stone Province in the world due to the amount, variety and quality of the exploited gem materials. The most important gemstones produced are agate and amethyst.

The state of Rio Grande do Sul concentrates a large number of agate-dyeing companies. The agate-dyeing process with organic dyes is carried out in plastic containers where the stones are placed into a dye alcoholic solution. After sometime, the stones are removed from the solution and washed with tap water. The effluent produced contains residual amounts of dyes and an intense colour [1, 2].

The dye wastewater discharge in water bodies is of environmental concern. Colored effluents are known to cause high oxygen demand, fluctuating pH, resistance to biological oxidation and prevents sunlight penetration, decreasing photosynthetic activity in aqueous environment.

Rhodamine B (RB) is one of main organic fluorescent dyes present in a typical Brazilian agate industry used to give an artificial colour pink to the stones. The general characteristics of RB are summarized in

Table 1 and the chemical structure is in Figure 1. It is also widely used as a colorant in textiles and food stuffs, water tracer fluorescent and in the production of printer cartridges inkjet and laser [3-6].

Table 1. General characteristics of dye Rhodamine B.

Generic number	CI 45107*
Chromophores groups	-C=C- / -C=N- / quinoid ring
Absorbance at the maximum wavelength (nm)	543-557
Molar mass (g mol ⁻¹)	479.02
Chemical formula	C ₂₈ H ₃₁ N ₂ O ₃ Cl
Ionization class	Basic
Chemistry class	Xanthene

*CI = Color Index

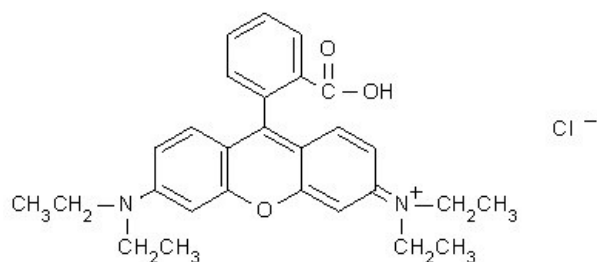


Figure 1. Chemical structure of Rhodamine B dye.

The RB is harmful to human beings and animals because can cause irritation of the skin, eyes and respiratory tract. Besides this, the carcinogenicity, reproductive and developmental toxicity, neurotoxicity and chronic toxicity toward humans and animals of this dye have been related in literature [7, 8].

The most common effluent treatment used by the Brazilian agate-dyeing industries is chemical oxidation with sodium hypochlorite. However, the use of sodium hypochlorite for the oxidation of the effluent causes the formation of chlorinated organic compounds [9].

Adsorption is one of the most effective methods for removal of dyes from effluents and constitutes an interesting alternative to chemical method [10, 11]. Conventional adsorbent such as activated carbons is highly effective, but the running costs and adsorbent purchase are high. Therefore, locally available and abundant materials could be used as a source for producing cost-effective adsorbent.

In the southwest of state of Rio Grande do Sul are located also the largest coal reserves in Brazil, as well as the Presidente Médici coal-fired Power Station. Brazilian coals are richer in ash (content of 20–50 wt.%) and poorer in carbon when compared to worldwide coal. Bottom ash does not find at present time a large commercial application and is disposed at lagoons near the site.

Zeolites from Brazilian coal ash have been used as an effective low-cost adsorbent in many applications. Moreover, a considerable reduction in the elements contents and in the toxicity to living organisms was attained in the fly ash zeolitization [12, 13].

Zeolites have permanent negative charges in their crystal structures, which enable them to be modified by cationic surfactants, such as, hexadecyltrimethylammonium. The modification of the zeolitic material enhances the removal of organic and anionic pollutants from effluents [14, 15].

The evaluation of the best adsorption conditions of dyes from aqueous solutions in different adsorbents has been studied by several researchers by using a factorial design technique. Factorial designs are used to investigate the principal experimental factors that might influence the dye adsorption and the interactions between those factors [16-19].

The objective of this study was use coal bottom ash as a starting material for surfactant-modified zeolite synthesis. The organozeolite was evaluated as adsorbent to remove Rhodamine B from aqueous solution. The influence of the most effective parameters in the adsorption process for dye removal (pH, temperature, adsorbent amount and initial dye concentration) was investigated using 2⁴ full factorial design. The reuse of the remaining solution generated from the synthesis of zeolite was also evaluated.

2. Materials and method

2.1 Materials

The reagents used for experimental studies were of analytical grade. Rhodamine B (RB) dye was obtained from Casa Americana company with a dye content of 100% and was used without further purification. The quaternary ammonium salt hexadecyltrimethylammonium bromide (HDTMA-Br, Merck) was used in the modification of zeolite. Sodium aluminate from Aldrich Company was used to zeolite the synthesis from the remaining solution. A stock solution of RB was prepared in double distilled water and the solutions for adsorption tests were prepared by diluting it. Mechanical shaker (Quimis – model Q-225M), centrifuges (Quimis – model Q-222), oven (Fanem Orion 515) and UV/Visible spectrophotometer (Varian – model Cary 1E) were used. The samples of coal bottom ash (CBA) were obtained from a coal-fired power station (Presidente Médici Power Plant or UTPM-446 MW) located at Candiota County, in Rio Grande do Sul State, Brazil.

2.2 Synthesis of zeolite

The Figure 2 shows a schematic drawing of all zeolite synthesis performed in this work.

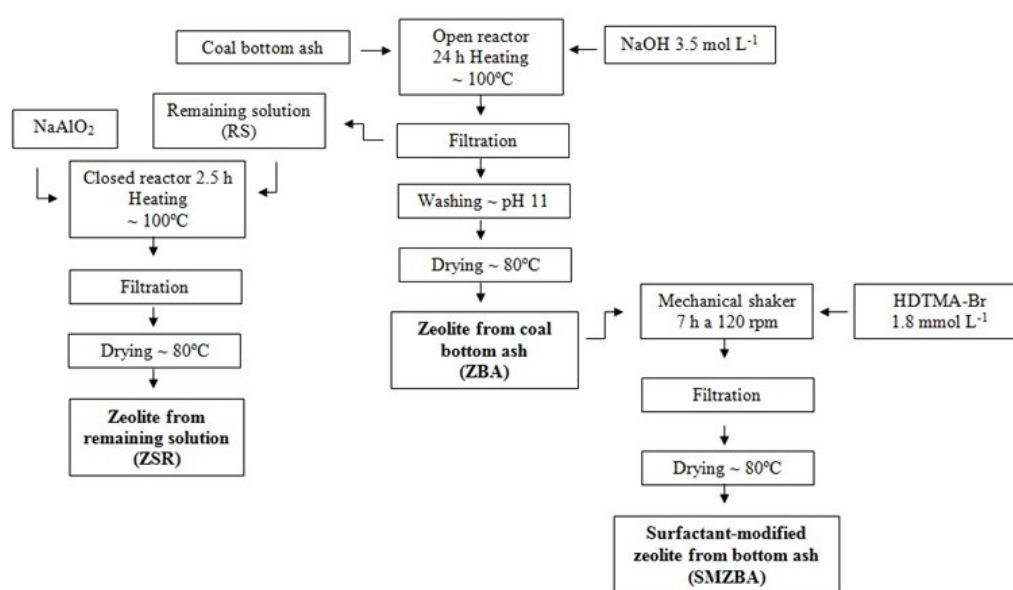


Figure 2. Synthesis scheme of zeolites.

2.2.1 Synthesis of zeolite from coal bottom ash

The zeolite (ZBA) prepared was with CBA (20 g) mixed with 160 mL of 3.5 mol L⁻¹ aqueous NaOH solution, this mixture was heated to 100 °C in oven for 24 h. After finishing of the process, the suspension was filtered with 4A quantitative filter paper and repeatedly washed with deionized water until the pH of washing water reach ~ 11 and dried at 80 °C for 12 h [20].

2.2.2 Synthesis of surfactant-modified zeolite from bottom ash

For the synthesis of zeolite modified, 10 g of ZBA were mixed with 200 mL of hexadecyltrimethylammonium bromide (HDTMA-Br) solution at concentration 1.8 mmol L⁻¹. The mixture of zeolite and HDTMA-Br solution was stirred for 7 h at 120 rpm and 25 °C. The suspension was filtered and the solid was dried in oven at 50 °C for 12 h [20]. Zeolite modified was named as SMZBA. The characterization of the ZBA and CBA that served as raw material in the synthesis is described in literature [21].

2.2.3 Synthesis of zeolite from remaining solution

The remaining solution (RS) obtained from the filtration after the hydrothermal treatment of CBA (item 2.2.1.) was characterized to determine the concentrations of Si and Al in the solution. The commercially important molecular sieve zeolites types presents a molar ratio of Si/Al ≈ 1, which is considered as highest aluminum content possible in tetrahedral aluminosilicate frameworks. The molar Si/Al ratio of RS was adjusted to 1.0 by adding Al³⁺ solution, prepared using 2.15 g of NaAlO₂ in 150 mL of

NaOH 3.5 mol L⁻¹ stirred for ~ 10 min at 25 °C. Then, 30 mL of RS were added to sodium aluminate solution and stirred for 2 min. The mixture was heated in an oven at 100 °C for 2.5 h. The suspension was filtered and the solid was washed repeatedly with bi-distilled water until pH ~ 11. The residue was dried at 80 °C for 12 h. A second synthesis was also tested by using only the mixture of water (150 mL) and RS (30 mL) in the alkaline hydrothermal treatment without addition of aluminum.

2.3 Characterization of materials

The chemical composition and morphology were determined by Scanning Electron micrograph/energy dispersive X-ray (SEM/EDS) using XL-30 Philips scanning electron microscope. The particle size of the materials was measured using a laser based particle size analyzer, namely a Malvern MSS Mastersizer 2000 Ver. 5.54. The mineralogical compositions were determined by X-ray diffraction analyses (XRD) with an automated Rigakumultiflex diffractometer with Cu anode using Co K α radiation at 40 kV and 20 mA over the range (2θ) of 5-80° with a scan time of 0.5°/min.

The cation exchange capacity (CEC) and external cation exchange capacity (ECEC) were determined according to the literature [22, 23].

The pH and the conductivity were measured as follows: samples (0.25 g) were placed in 25 mL of deionized water and the mixture was stirred for 24 h in a shaker at 120 rpm (Ética - Mod 430). After filtration, the pH of the solutions was measured with a pH meter (MSTecnopon - Mod MPA 210) and the conductivity was measured with a conductivimeter (BEL Engineering - Mod W12D).

To determine the point of zero charge (pH PZC) of the ZBA and SMZBA, 0.1 g of sample were placed in 50 ml of sodium nitrate (0.1 mol L⁻¹) and the mixtures were shaken for 24 h on the mechanical shaker (Quimis - MOD Q - 225M) at 120 rpm. The solutions were adjusted to initial pH values of 2, 4, 10, 11, 12 and 13 by adding 0.1 and 1 mol L⁻¹ HCl or 3 mol L⁻¹ NaOH solution. The difference values between the initial and final pH (pH Δ) were placed in a graph in function of the initial pH. The point x where the curve intersects the y = 0 is the pH PZC.

The bulk density and the specific surface area was determined by a helium picnometer (Micromeritics Instrument Corporation - Accupyc 1330) and by a BET Surface Area Analyser (Quanta chrome Nova - 1200), respectively. Prior to determination of the specific surface area, samples were heated at 423.15 K for 12 h to remove volatiles and moisture in a degasser (Nova 1000 Degasser). The BET surface areas were obtained by applying the BET equation to the nitrogen adsorption data. The Fourier transform infrared spectroscopy (FTIR) spectra were recorded on Nexus 670 Thermo Nicolet using KBr pellet method.

2.4 Adsorption studies

Studies to remove the dye by surfactant-modified zeolite were accomplished by stirring discontinuous processes. Aliquots of 10 mL of RB with initial concentrations 5, 10 and 20 mg L⁻¹ were placed in beakers with 0.1 g of SMZBA. The suspensions were shaken at 120 rpm at intervals of 5-120 min (25 \pm 2 °C). The supernatant was separated by centrifugation for 5 min at 3000 rpm. An aliquot of the supernatant was analyzed using a UV spectrophotometer by measuring absorbance at 554 nm.

The amount of the dye uptake and percentage of dye removal by the adsorbent were calculated by applying equation (1) and (2), respectively:

$$q = \frac{V(C_0 - C_t)}{M} \quad (1)$$

$$R = \frac{100(C_0 - C_t)}{C_0} \quad (2)$$

where q_t is the adsorbed amount of adsorbate per gram of adsorbent at any time t (mg g⁻¹), C_0 and C_t the concentrations of the adsorbate in the initial solution and at any time t , respectively (mg L⁻¹); V the volume of the adsorbate solution added (L) and M the amount of the adsorbent used (g).

In order to investigate the transient mechanism of adsorption, characteristic constants were determined using the linearized form of pseudo-first order [24] and pseudo-second order [25]. The linearized equations of the models and their corresponding graphs are shown in Table 2.

The data from the adsorption equilibrium isotherms were analyzed using Langmuir, Freundlich, Temkin and Dubinin-Radushkevich (D-R) [26]. The nonlinearized mathematical expressions models of isotherms and their line graphs are given in Table 3.

Table 2. Linear equations and graphs of kinetic models.

Model	Equation	Graphic
pseudo-first order	$\log(q_e - q_t) = \log q_e - k_1 t$	$\log (q_e - q_t)$ vs t
pseudo-second order	$\frac{1}{q_t} = \frac{1}{k_2 q_e^2} + \frac{t}{q_e}$	t/q_t vs t

Table 3. Nonlinearized mathematical expressions models of isotherms.

Model	Equation	Parameters
Langmuir	$q_e = \frac{(Q_o \cdot b_L \cdot C_e)}{(1 + b_L \cdot C_e)}$	q_e – amount of adsorbate in the adsorbent at equilibrium C_e – equilibrium concentration Q_o – Maximum capacity of adsorption at equilibrium b_L – Langmuir isotherm Constant
Freundlich	$q_e = k_F \cdot (C_e)^{1/n}$	k_F – Freundlich constants n – adsorption intensity
Temkin	$q_e = B_T \ln (k_T C_e)$	k_T – Tempkin isotherm equilibrium binding constant B_T – Tempkin isotherm constant
D-R	$q_e = k_{D-R} \exp^{-\beta \varepsilon^2}$ $\varepsilon = RT \ln (1 + C_e^{-1})$	k_{D-R} – theoretical isotherm saturation capacity β – Dubinin–Radushkevich isotherm constant ε – Dubinin–Radushkevich isotherm constant R – universal gas constant (8.314 J mol ⁻¹ K ⁻¹) T – temperature (K)

In assessing the best fit of the models to the experimental data will have a closer to zero, X^2 values for nonlinear equations. In addition were analyzed 6 estimated deviation, and the lower values will be used to further validate the applicability of the tested isotherms. The used equations shown in Table 4 (abbreviated as ARED, SSE, MPSED, HYBRID, SAE and X^2) are described in the literature [26-29].

Table 4. Equations of deviation estimates

Error function	Expression ⁽¹⁾
Average relative error	$ARE = \frac{100}{N} \sum \left \frac{q_{eexp} - q_{ecal}}{q_{eexp}} \right $
Marquardl standard deviation percentage	$MPSD = 100 \sqrt{\frac{1}{N - P} \sum \left \left(\frac{q_{eexp} - q_{ecal}}{q_{eexp}} \right)^2 \right }$
Hybrid function fractional	$HYBRID = \frac{100}{N - P} \sum \left \frac{q_{eexp} - q_{ecal}}{q_{eexp}} \right $
Sum of squared errors	$SSE = \sum (q_{ecal} - q_{eexp})^2$
Error estimate of the sum	$SAE = \sum q_{eexp} - q_{ecal} $
Chi-square	$X^2 = \sum \frac{(q_{eexp} - q_{ecal})^2}{q_{ecal}}$

(1) q_{eexp} = amount of adsorbate in the adsorbent at equilibrium, in mg g⁻¹; q_{ecal} = amount of adsorbate in the adsorbent at calculated in mg g⁻¹

2.5 Factorial design

The four factors temperature, pH, adsorbent dosage and initial concentration of the dye are varied at three levels as shown in the Table 5. For each run, 10 mL of dye solution taken in flasks together with the adsorbent SMZBA were agitated at 120 rpm for 1 h. After one hour of contact time samples were then centrifuged (3000 rpm during 5 min) and the concentration in the supernatant solution was analyzed using a UV spectrophotometer (Cary 1E, Varian) at a maximum wavelength of 554 nm. Eighteen experiments with all possible combinations of variables were conducted, and a matrix was established according to their high, center and low levels, represented by +1, 0 and -1, respectively.

Table 5. High and low levels of factors.

Factor	High level (+1)	Center level (0)	Low level (-1)
(A) Temperature	45	35	25
(B) pH	8	5	2
(C) Adsorbent dosage	0.5	0.3	0.1
(D) Concentration of the dye	20	15	10

3. Results and discussion

3.1 Synthesis of zeolite from remaining solution

The remaining solution (RS) of classical alkaline hydrothermal treatment of bottom ash is usually discarded after recovering the zeolite crystals, although it may contain valuable chemicals that can facilitate further growth of nanocrystalline zeolites. Large quantities of Si^{4+} and a minor amount of Al^{3+} are present in the supernatant waste of synthesis because mullite is more stable than quartz in alkaline solution [30, 31].

The color of the product formed after the treatment of waste solution was white, different from gray of original bottom ash and their zeolite indicating that the main elements of material are Si, Al, O and Na [31].

The observed (Figure 3) peaks with d-spacing values of 14.7, 25, 35.7, 53.9, 59, 61 and 63° are ascribed to formation of zeolite hydroxysodalite (JCPDS 011-0401). The mineral phase mullite was also present in the solid product. This result shows that the aluminum added to the reaction mixture did not react completely during the formation of the zeolite at the conditions used in these assays, probably needing longer times.

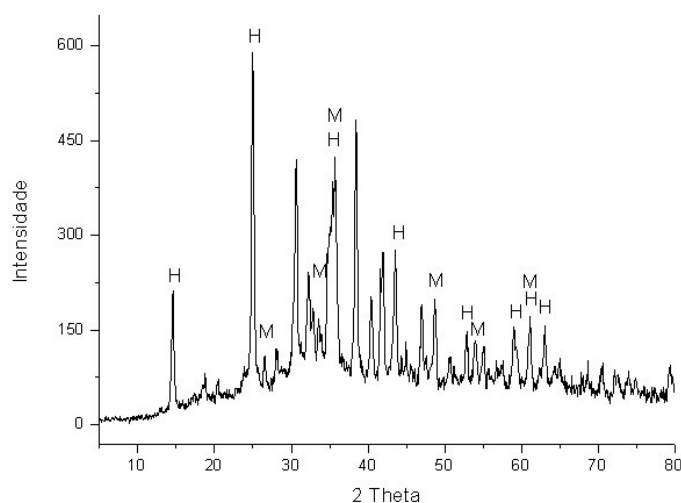


Figure 3. X-ray diffraction patterns of the zeolite from remaining solution (M = Mullite; H = Hydroxysodalite).

Hydrothermal treatment conducted without addition of aluminum resulted in no zeolite-like materials. The amount of Al^{3+} ions dissolved into the alkaline solution during alkaline treatment was not sufficient to condense to form an alumina-silicate gel, which is pre-material of zeolite crystal covering the outer surface of bottom ash. Therefore, the addition of the alkaline aluminum solution in the supernatant waste was indispensable for preparing zeolitic compound.

3.2 Characterization of materials

3.2.1 Energy Dispersive Spectroscopy (EDS) analysis

Energy dispersive X-ray spectroscopy (EDS) was used for elemental analysis of the materials. The EDS spectrum in Figure 4 confirmed the presence of Si and Al which are mainly elements in CBA involved in creating the structure of zeolite.

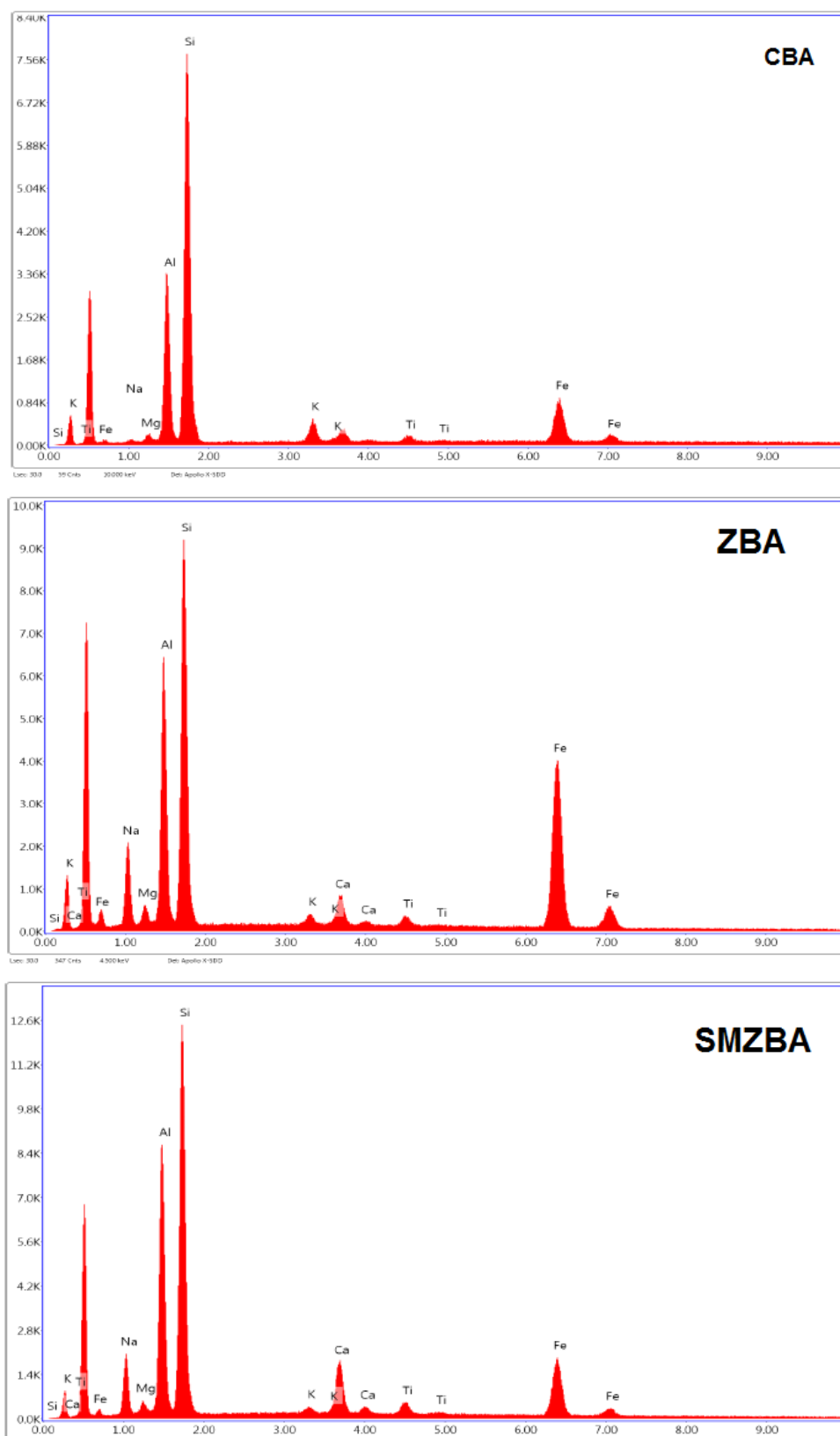


Figure 4. EDS spectra of the CBA, ZBA and SMZBA materials.

EDS spectra of the studied samples ZBA and SMZBA show also strong elemental signal of iron and sodium. It can be seen that both CBA, ZBA and SMZBA materials has impurities existing as calcium, titanium, magnesium and iron elements. For SMZBA, sodium is the main exchange cation in the structure balancing the charge of the aluminosilicate lattice.

Table 6 represents the weight percentages of occurrence elements in bottom ash raw material and organozeolites powder. The main components of CBA are silicon (Si), aluminium (Al) and iron (Fe). Elements of potassium, titanium, magnesium and others were found in amounts equal to or lower than 4wt%. For the nanozeolites materials ZBA and SMZBA, the chemical compositions are mainly silicon, aluminium and iron. The significant amount of Na incorporated in the final products is the result of alkaline treatment with NaOH [30].

The resulting Al/Si ratio of the modified zeolite is 0.533 which is fairly close to that of the untreated zeolite (0.618). This indicates that the Al atoms were not lost into the aqueous media during surface modification with surfactant.

Previous study with analysis of coal, fly ash and bottom ash from Presidente Médici Power Plant was reported. The fly and bottom ashes were characterized by relatively high contents of SiO₂ (56-59%) and Al₂O₃ (36-38%) and low contents of alkaline oxides. Trace Elements were classified into three groups based on their content in fly and bottom ashes, and enrichments or depletions of these element in relation to the coal [32].

Table 6. Weight percentages of occurrence elements in coal bottom ash, unmodified and modified surfactant zeolitic materials.

Elements	CBA (%)	ZBA (%)	SMZBA (%)
Si	60.17	34.78	44.98
Al	19.79	21.49	23.97
Fe	14.95	24.87	12.23
K	3.95	0.71	0.65
Ti	0.98	0.77	1.62
Mg	0.16	1.72	0.56
Na	-	13.23	9.26
Ca	-	2.44	6.72

3.2.2 Scanning electron microscopic analysis

The morphology of the starting material, zeolitic material and surfactant-modified zeolitic material were observed by scanning electron microscopy. Figure 5 (a), (b) and (c) show the scanning electron microscopy images of CBA, ZBA and SMZBA, respectively at a magnification of x1000. At this range, hollow cenospheres were detected along the surface of the bottom ash samples at different sizes, with a smooth surface made of an aluminosilicate glass phase (Figure 5(a)). The surface became rough due the deposition of zeolite crystals on the bottom ash particles after hydrothermal treatment (Figure 5 (b and c)). The modification of the zeolite with HDTMA causes no significant difference in their SEM image due the HDTMA only bonds on the surface of the zeolite without to cause changes in the morphology [33].

3.2.3 Physicochemical properties

Table 7 presented the physicochemical properties of the materials used in this investigation. The specific surface area value of the surfactant-modified zeolitic material (67.8m² g⁻¹) was ~ 27 times greater than those of bottom ash. The increase in the specific surface area of bottom ash after hydrothermal treatment confirmed the formation of zeolitic phases. Zeolites have high porosity and present channels and cavities, which contribute to their high values of specific surface area [34].

The bulk density value of CBA corresponds to material containing particles with high glass phase of quartz and mullite [35-38]. The bulk density value of zeolites is also generally between 2- 2.4 g cm⁻³ and can correlate with its porosity and cation exchange capacity [39].

The pH value of CBA (7.5) indicates that coal ash was lightly alkaline in nature due the presence of alkali and alkaline earth cations combined with carbonates, oxides or hydroxides [40, 41]. The high pH of zeolitic materials is attributed to entrapment of sodium ions to neutralize the negative charge on aluminosilicate gel during the hydrothermal treatment.

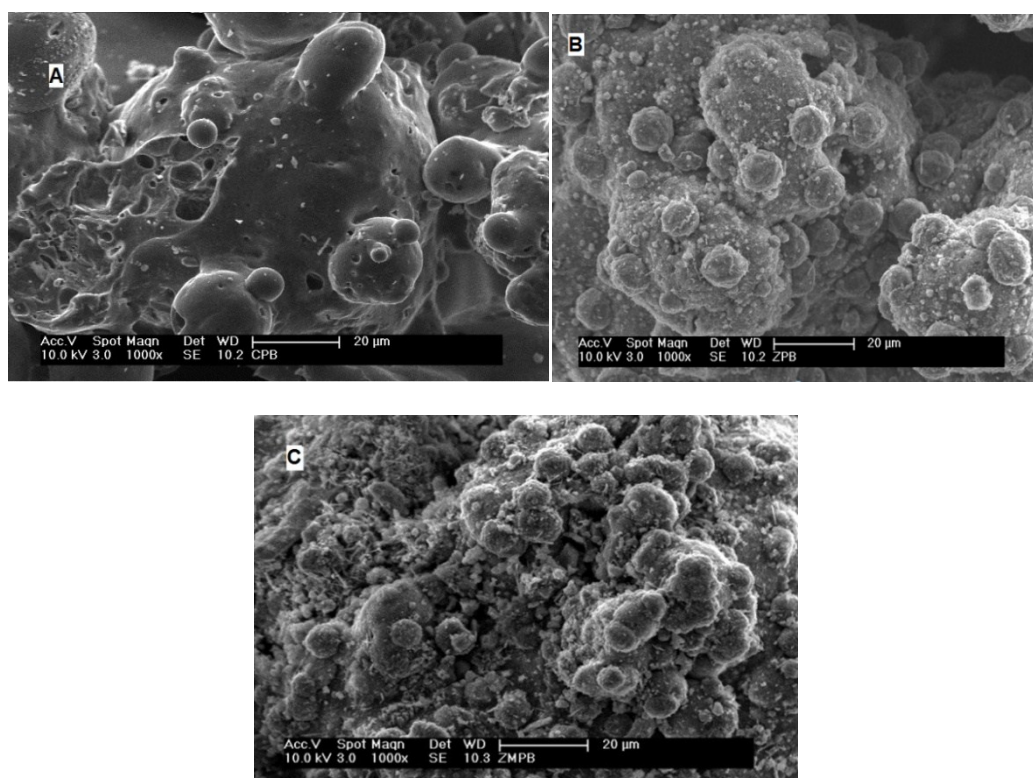


Figure 5. SEM photographs of (a) CBA; (b) ZBA; (c) SMZBA. Magnification 1000x.

Table 7. Physicochemical properties of coal bottom ash (CBA) and zeolitic products.

Properties	CBA	ZBA	SMZBA
Specific surface area ($\text{m}^2 \text{g}^{-1}$)	2.5	-	67.8
Bulk density (g cm^{-3})	1.98	-	2.30
pH in water	7.5	9.7	9.5
$\text{pH}_{\text{PZC}}^{\text{c}}$	-	7.4	8.2
Conductivity ($\mu\text{S cm}^{-1}$)	43.8	694	542
CEC (meq g^{-1}) ^a	0.161	2.16	1.99
ECEC (meq g^{-1}) ^b	-	0.603	-

(a) cation exchange capacity; (b) external cation exchange capacity; (c) point of zero charge

The pH_{pzc} value is an important indicator of the net surface charge and the preference for the ionic species for an adsorbent. The results of the determination of the pH_{pzc} were 7.4 and 8.2 for ZBA and SMZBA, respectively. For both materials, the pH in water is higher than pH_{pzc} indicating that their surfaces have negative charge in aqueous solution. SMZBA has negative charge probably due to the formation of a patchy mono-layer and/or bi-layers form on the number of exchangeable active sites on the external zeolite surface [20].

The conductivity values are related to some compounds present in coal ash and in zeolitic products that can undergo dissolution. Conductivity values of the zeolites were higher than the bottom ash samples due to the presence of exchangeable cations in their structures formed by the hydrothermal treatment. The results are in agreement with other studies that reported the values of conductivity for different Brazilian bottom ashes and their respective zeolites [34].

Also, the CEC values of the zeolitic materials were ~ 10 times higher than the value of CBA because the Si/Al ratio, which is associated to the cation exchange capacity, change after the hydrothermal treatment. The CEC of zeolitic material was not affected by the presence of the surfactant on the surface because the sites occupied by the surfactant molecules are not considered in the determination. The external cation exchange capacity (ECEC) of SMZBA accounts for 28 % of CEC.

The particle size distributions obtained for bottom ash is shown in Figure 6. The distributions specify that the majority of particles (90%) lie below 654.448 μm and continuous interval of particle size was between 11.3 to 1261.9 μm .

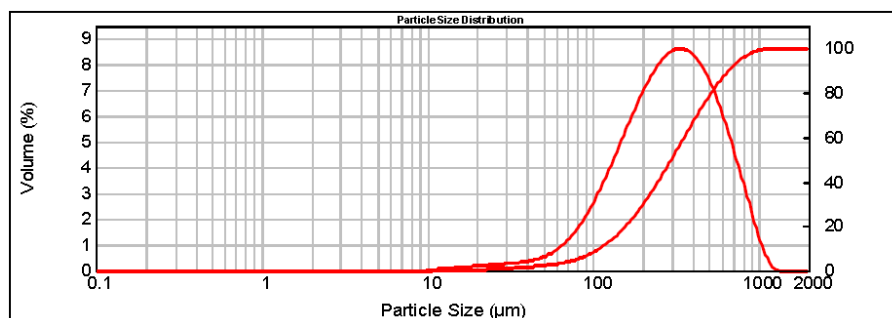


Figure 6. Particle size distribution of the CBA.

3.2.4 FTIR spectroscopy

FTIR spectra of the CBA, ZBA and the SMZBA are shown in Figure 7. The broad bands at approximately 3450 cm^{-1} and the peaks at about 1650 cm^{-1} are for O–H stretching and O–H bending, respectively. For zeolitic materials, these bands can also be related to the water molecules located inside the channels of zeolites and/or associated with exchangeable cations [42].

For CBA, the peak at 1089 cm^{-1} is attributed to the Si–O–Si and Si–O–Al asymmetric stretching, and the peak at 459 cm^{-1} is linked to the Si–O and Al–O in-plane flexural vibration modes. The peak at 794 cm^{-1} is due to symmetric stretching vibrations of SiO_4 [43, 44].

The IR pattern of ZBA and SMZBA shows the characteristic peaks at wave numbers $3442\text{--}3456$, $1641\text{--}1647$, 997 , 557 , and 465 cm^{-1} reported for zeolite-P and hydroxysodalite [45].

The peaks at 2924 and 2852 cm^{-1} observed in SMZBA can be assigned to HDTMA-Br adsorbed on the zeolite surface as the corresponding peaks are also observed in the IR pattern of HDTMA-Br only. These peaks are indicative of stretching vibrations of the $-\text{CH}_2$ and $-\text{CH}_3$ groups of HDTMA [46].

The presence of characteristic peaks of zeolite-P and hydroxysodalite for SMZBA confirms the structural stability of zeolite after surfactant modification.

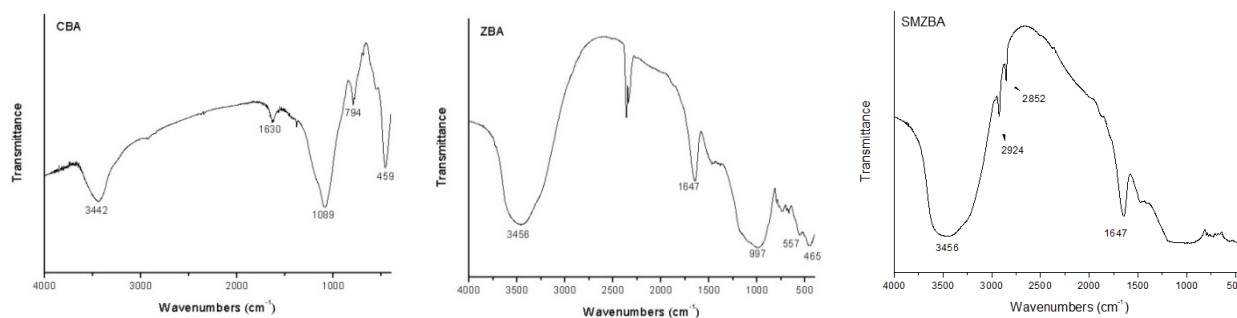


Figure 7. FTIR Spectra of raw coal bottom ash (CBA), unmodified zeolite (ZBA) and surfactant-modified zeolite (SMZBA).

3.2.5 Mineralogical compositions

Figure 8 shows the XRD patterns of the coal bottom ash (CBA), unmodified zeolite (ZBA) and surfactant-modified zeolite from bottom ash (SMZBA). The majority crystalline phases in the CBA were quartz (SiO_2 , ICDD/JCPDS 001-0649) and mullite (Al_2O_3 , ICDD/JCPDS 002-043) as expected.

Na-P1 ($\text{Na}_6\text{Si}_{10}\text{Al}_6\text{O}_{32}\cdot 2\text{H}_2\text{O}$, ICDD/JCPDS39-0219) and Hydroxysodalite (JCPDS 31-1271) were the main zeolitic products obtained after conventional alkaline hydrothermal activation of CBA. In addition to the presence of peaks characteristic of zeolites, residual quartz and mullite are also observed.

The structural parameters of the surfactant-modified zeolite are very close to that of corresponding unmodified, indicating that the crystalline nature of the zeolite remained intact after modification with surfactant [20].

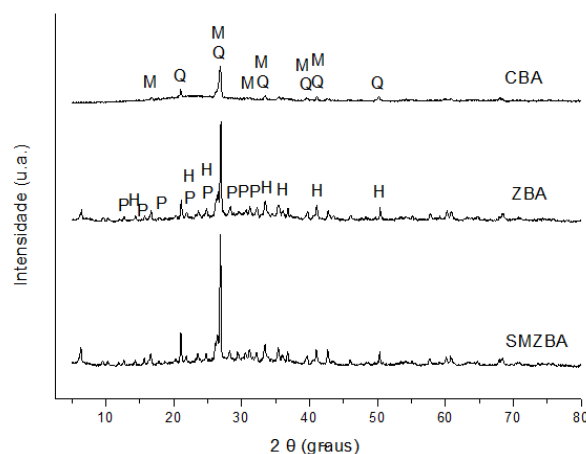


Figure 8. X-ray diffraction patterns of CBA, ZBA and SMZBA (M = Mulinite; Q = Quartz; H = Hydroxysodalite; P= NaP1).

3.3 Adsorption studies

The effect of time of agitation and initial concentration on the adsorption of dye by organozeolite were investigated for SMZBA/RB system (Figure 9). The removal of RB was very rapid in the first 10 min of contact time and after this period the rate of removal be slower and stagnates in 40 min.

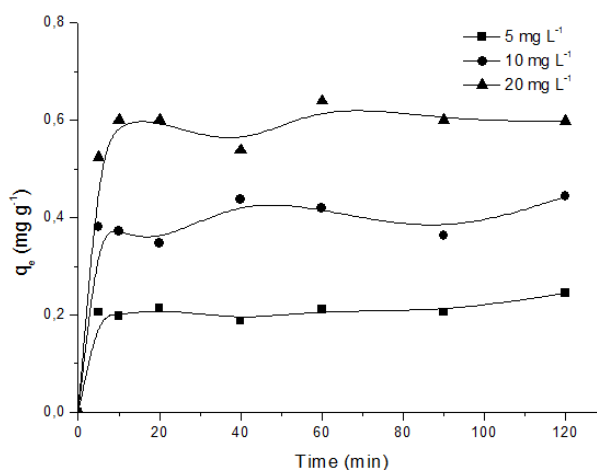


Figure 9. Effect of agitation time in the RB adsorption capacity by SMZBA ($T = 25 \pm 2^\circ\text{C}$).

The adsorption experiments were also conducted with coal bottom ash (CBA) and zeolite from coal bottom ash (ZBA) at the same conditions used with SMZBA, but as expected, little adsorption of RB by these two materials was observed. This indicates that adsorption of RB was mainly due to the loaded surfactant bilayer on zeolite surface.

In order to characterize the kinetics involved in the process of adsorption, two widely used kinetic models, pseudo-first-order and pseudo-second-order kinetic models, were analyzed based on the regression coefficient, (R^2) and the amount of dye adsorbed at equilibrium determined experimentally ($q_{e,exp}$). The values of the rate constants and the calculated q values ($q_{e,calc}$) are presented in Table 8. The R^2 value obtained was very high ($R \geq 0.99$) and the calculated q value was in accordance with the experimental one, further confirming that the adsorption of RB on SMZBA conformed to the pseudo-second order kinetic model.

The adsorption isotherms for RB onto SMZBA are shown in Figure 10, where the experimental values and curves achieved from the values estimated by the Langmuir, Freundlich, Temkin and D-R models are presented.

Upon applying the uptake classification scheme developed previously by Giles, et al., 1960 [47], the isotherm profiles of RB/SMZBA system obey the L3 pattern. The curve shows a straight portion following an inflection point. The turning point represents the development of a second layer and may

represent a change in mode of packing of the dye. The dye removal for RB was 30 to 50% with standard deviation of 3.13%.

The parameters of the Langmuir isotherm, Freundlich, Temkin and D-R for RB/SMZBA system were determined by nonlinear regression and are listed in Table 9.

Table 8. Kinetics parameters for RB removal onto SMZBA.

Pseudo-first order					
[RB] mg L ⁻¹	k ₁ (min ⁻¹)	q _e calc (mg g ⁻¹)	q _e exp (mg g ⁻¹)	R ² _{1a}	
5	4.24 x 10 ⁻³	0.011	0.211	0.219	
10	4.21 x 10 ⁻³	0.064	0.438	0.251	
20	4.40 x 10 ⁻³	0.069	0.640	0.405	
Pseudo-second order					
[RB] mg L ⁻¹	k ₂ (g mg min ⁻¹)	h (mg g min ⁻¹)	q _e calc (mg g ⁻¹)	q _e exp (mg g ⁻¹)	R ² _{2a}
5	1.02	0.056	0.235	0.211	0.990
10	1.17	0.208	0.422	0.419	0.989
20	2.52	0.922	0.605	0.640	0.998

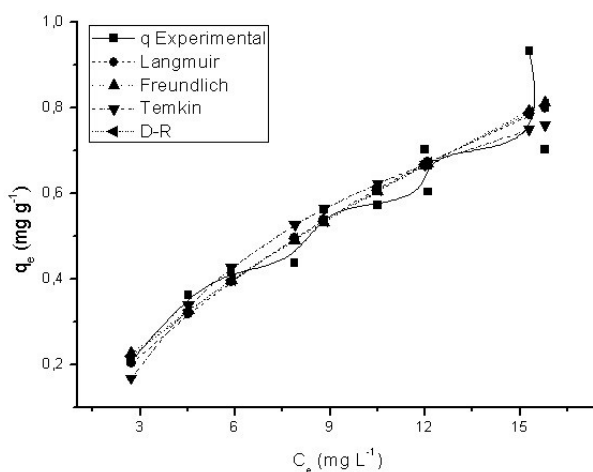


Figure 10. Adsorption isotherm of RB onto SMZBA (T =25 ± 2°C).

Table 9. Parameters of the Langmuir, Freundlich, Temkin and DR models for adsorption of RB onto SMZBA.

Langmuir	Parameters
Q ₀ (mg g ⁻¹)	2.03
b (L mg ⁻¹)	0.041
Freundlich	
k _F (mg g ⁻¹)(Lm g ⁻¹) ^{1/n}	0.110
n	1.38
Temkin	
k _T (L g ⁻¹)	0.609
B _t	0.336
b (kJ mol ⁻¹)	7.34
DR	
k _{DR} (mol g ⁻¹)	5.65 x 10 ⁻⁵
β (mol ² J ⁻²)	5.37 x 10 ⁻⁹
E (kJ mol ⁻¹)	9.65

The isotherm models Temkin and D-R are related to the energy involved in the adsorption process. Temkin isotherm model considers the heat of sorption of all the molecules in the layer would decrease linearly with coverage due to sorbate/sorbent interactions [26, 48]. The parameter b (J mol^{-1}) is the Temkin isotherm constant linked to the energy parameter, B , as shown on equation:

$$b = \frac{RT}{B} \quad (3)$$

D-R model has been used to describe the adsorption mechanism from a Gaussian distribution in heterogeneous surfaces [26]. The constant B gives the mean free energy E of sorption per molecule of the adsorbate when it is transferred to the surface of the solid from infinity in the solution and can be computed by using the relation:

$$E = \frac{1}{\sqrt{2\beta}} \quad (4)$$

It is well known that for diluted solutions the thermodynamic equilibrium constant of adsorption would be reasonably approximated by the Langmuir equilibrium constant (K_L), and thus the use of the Langmuir equilibrium constant for calculation of Gibbs standard free energies of adsorption (ΔG^0) is acceptable [49]. The free energy value was evaluated as $-24.5 \text{ kJ mol}^{-1}$ and can be inferred from the negative values that the adsorption process of RB onto SMZBA occurs spontaneously.

The values of error analysis for Langmuir, Freundlich, Temkin and D-R isotherm models are presented in Table 10. When more than two models are compared, from the non-linear regression are considered the lowest values of each deviation estimate (ARE, SSE, MPSD, HYBRID, SAE and X^2).

Table 10. Error functions analysis related to the adsorption of RB onto SMZBA.

Modelo	ARE	SSE	MPSD	HYBRID	SAE	X^2
Langmuir	9.02	0.045	11.3	11.3	0.540	0.067
Freundlich	9.28	0.044	11.2	11.6	0.539	0.063
Temkin	10.1	0.055	13.7	12.6	0.554	0.088
D-R	8.97	0.044	11.0	11.2	0.533	0.063

The results showed that D-R model that best describes the system under study, it has the lowest values of deviation estimates, indicating predominantly homogeneous distribution of active sites on the SMZBA surface, since the D-R equation assumes that the adsorbent surface is energetically homogeneous.

3.4 Factorial design

The results were analyzed using MINITAB 17 for Windows. The effect of a factor is the change in response, here, adsorption capacity of organomodified zeolite produced by a change in the level of a factor, temperature, pH, adsorbent dosage and initial concentration of the dye from three levels. The main effects and interaction between factors were determined. The factorial design matrix and q_e measured in each factorial experiment is shown in Table 11.

The effects, regression coefficients, standard errors, T and P are shown in Table 12. Figure 11 shows the main effects of the four factors on adsorption capacity of SMZBA. The main effects represent deviations of the average between high and low levels for each one of them. When the effect of a factor is positive, adsorption capacity of SMZBA increase as the factor is changed from low to high levels. In contrast, if the effects are negative, a reduction in adsorption capacity of SMZBA occurs for high level of the same factor [18].

The effects of adsorbent dosage and initial concentration factors are negative and positive, respectively. Maximum adsorption occurred in the low dose and high adsorbent dye initial concentration. The expression (Equation (5)) describes how the experimental variables and their interactions influencing the adsorption of the dye [50]:

$$n = F_0 + F_1X_1 + F_2X_2 + F_3X_3 + F_4X_4 + F_5X_1X_2 + F_6X_1X_3 + F_7X_1X_4 + F_8X_2X_3 + F_9X_2X_4 + F_{10}X_3X_4 + F_{11}X_1X_2X_3 + F_{12}X_1X_2X_4 + F_{13}X_1X_3X_4 + F_{14}X_2X_3X_4 + F_{15}X_1X_2X_3X_4 \quad (5)$$

Where F_0 represents the global mean and F_i represents the regression coefficient corresponding to the main factor effects and interactions. Substituting the regression coefficients in equation (5) we get model equation relating the level of parameters and color adsorption capacity.

$$n = 0.43875 + 0.01625A - 0.01237B - 0.18950C + 0.16013D + 0.00087AB - 0.01300AC - 0.01113AD + 0.00587BC + 0.00500BD - 0.06687CD + 0.00663ABC - 0.00050ABD + 0.00938ACD - 0.01050BCD + 0.01000ABCD \quad (6)$$

The adsorbent dosage (C) had the greatest effect on q_e followed by initial concentration (D), adsorbent dosage-initial concentration interaction (CD).

Table 11. Design matrix and the results of the 2^4 full factorial design.

Experiment	A	B	C	D	$q_e(\text{mg g}^{-1})$
1	-1	-1	-1	-1	0.390
2	+1	-1	-1	-1	0.313
3	-1	+1	-1	-1	0.833
4	+1	+1	-1	-1	0.860
5	-1	-1	+1	-1	0.150
6	+1	-1	+1	-1	0.152
7	-1	+1	+1	-1	0.370
8	+1	+1	+1	-1	0.312
9	-1	-1	-1	+1	0.480
10	+1	-1	-1	+1	0.422
11	-1	+1	-1	+1	0.883
12	+1	+1	-1	+1	0.845
13	-1	-1	+1	+1	0.164
14	+1	-1	+1	+1	0.158
15	-1	+1	+1	+1	0.339
16	+1	+1	+1	+1	0.349
17	0	0	0	0	0.365
18	0	0	0	0	0.388

Table 12. Statistical parameters for 2^4 design.

Term	Effects	Coefficients	Standard error	T	P
Constant		0.43875	0.00407	107.91	0.006
T	0.03250	0.01625	0.00407	4.00	0.156
pH	-0.02475	-0.01237	0.00407	-3.04	0.202
M	-0.37900	-0.18950	0.00407	-46.61	0.014
C	0.32025	0.16013	0.00407	39.38	0.016
T*pH	0.00175	0.00087	0.00407	0.22	0.865
T*M	-0.02600	-0.01300	0.00407	-3.20	0.193
T*C	-0.02225	-0.01113	0.00407	-2.74	0.223
pH*M	0.01175	0.00587	0.00407	1.44	0.385
pH*C	0.01000	0.00500	0.00407	1.23	0.435
M*C	-0.13375	-0.06687	0.00407	-16.45	0.039
T*pH*M	0.01325	0.00663	0.00407	1.63	0.350
T*pH*C	-0.00100	-0.00050	0.00407	-0.12	0.922
T*M*C	0.01875	0.00938	0.00407	2.31	0.261
pH*M*C	-0.02100	-0.01050	0.00407	-2.58	0.235
T*pH*M*C	0.02000	0.01000	0.00407	2.46	0.246

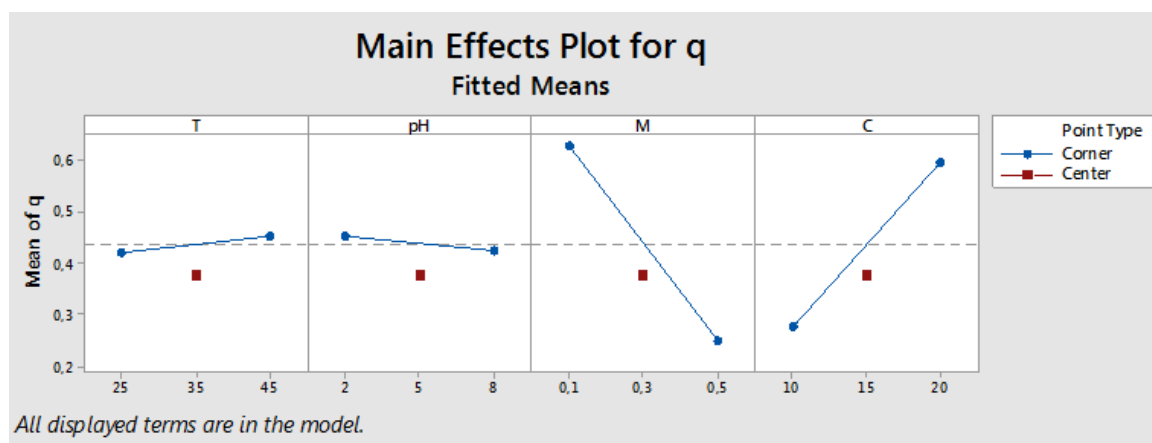


Figure 11. Main effects plot for adsorption capacity of SMZBA (mg g^{-1}).

The values for each effect are shown in Pareto chart (Figure 12) by horizontal columns and student's t-test was performed to determine whether the calculated effects were significantly different from zero. The Pareto chart gives the relative importance of the individual and interaction effects. The vertical line in the chart indicates the minimum statistically significant effect magnitude for 95% confidence level. For a 95% confidence level t-value is equal to 12.71.

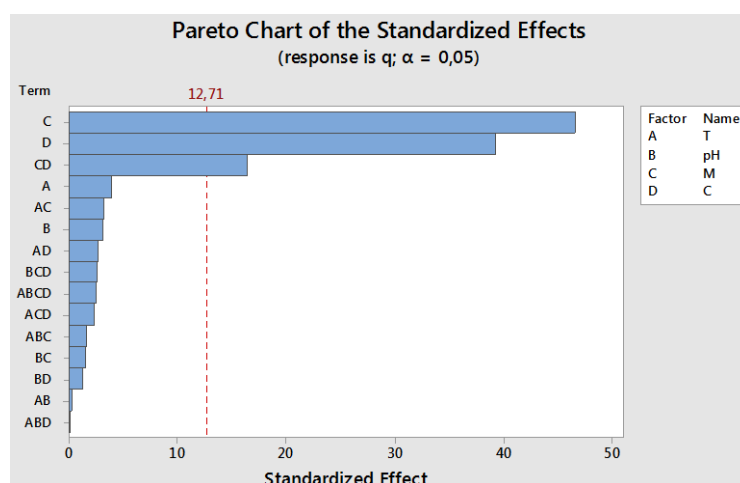


Figure 12. Pareto chart of standardized effects on the adsorption capacity for system SMZBA/RB.

The significance of the regression coefficients was determined by applying a Student's t-test. Three effects were significant with 95% confidence level, adsorbent dosage, initial concentration and interaction of the two. In addition, the model presented an adjusted square correlation coefficient R^2 (adj) of 99.58%, fitting the statistical model quite well.

According to the ANOVA table (Table 13), $P < 0.05$ for the main factors and their 2-way interactions, and the R^2 value for q_e was 0.9998, which was a desirable figure. The two studied variables must be manipulated at the lowest levels of adsorbent dosage but at the highest level of initial concentration (–, +).

The sum of squares being used to estimate the factors' effect and the F-ratios, which are defined as the ratio of the respective mean-square-effect to the mean-square-error is show in Table 13. The significance of these effects was evaluated using the t-test, and had a significance level of 5%; i.e., with a confidence level of 95%. The R-squared statistic indicated that the first-order model explained 99.98% of q_e 's variability. From the P-value, defined as the lowest level of significance leading to the rejection of the null hypothesis, it appears that the main effect of each factor and the interaction effects were statistically significant: $P < 0.05$ [51]. The results revealed that the studied factors (C and D) and their 2-way interaction (CD) were statistically significant to q_e .

Table 13. Analysis of variance (ANOVA) for adsorption capacity for system SMZBA/RB.

Source	Degrees of freedom	Sum of squares (SS)	Mean square (MS)	F	P-value
T	1	0.00423	0.004225	15.97	0.156
pH	1	0.00245	0.002450	9.26	0.202
M	1	0.57456	0.574564	2172.26	0.014
C	1	0.41024	0.410240	1551.00	0.016
T*pH	1	0.00001	0.000012	0.05	0.865
T*M	1	0.00270	0.002704	10.22	0.193
T*C	1	0.00198	0.001980	7.49	0.223
pH*M	1	0.00055	0.000552	2.09	0.385
pH*C	1	0.00040	0.000400	1.51	0.435
M*C	1	0.07156	0.071566	270.53	0.039
T*pH*M	1	0.00070	0.000702	2.66	0.350
T*pH*C	1	0.00000	0.000004	0.02	0.922
T*M*C	1	0.00141	0.001406	5.32	0.261
pH*M*C	1	0.00176	0.001764	6.67	0.235
T*pH*M*C	1	0.00160	0.001600	6.05	0.246
Model	16	1.08105	0.067566	255.45	0.049

$S = 0.0162635$; $R^2 = 99.98\%$; R^2 (adj) = 99.58%; $F = \text{adj. MS}_{\text{Factor}}/\text{adj. MS}_{\text{Error}}$.

4. Conclusion

The present study demonstrated that the surfactant-modified zeolite synthesized from coal bottom ash (SMZBA) is an effective adsorbent for removal of Rhodamine B (RB) from aqueous solution. Physical-chemical analysis confirmed the formation of mixed monolayer and double-layer surfactant on zeolitic material surface. Kinetic and equilibrium adsorption data were best represented by the pseudo-second order kinetic model and D-R isotherm model, respectively. The formation of zeolite using the remaining solution from the hydrothermal treatment of bottom ash was effective. Finally, the main effects on adsorption of RB onto SMZBA (temperature, pH, adsorbent dosage and initial concentration of the dye) and interaction between factors were determined. Three effects were significant with 95% confidence level, adsorbent dosage > initial concentration > interaction of the two.

Acknowledgements

The authors thank the National Council for Scientific and Technological Development (CNPq), Brazil for the financial support and President Médici Thermal Power Plant for supplying the coal ash samples.

References

- [1] Barros, A. L., Pizzolato, T. M., Carissimi, E., Schneider, I. A. H. Decolorizing dye wastewater from the agate industry with Fenton oxidation process. *Minerals Engineering*. 2006, 19 (1), 87-90.
- [2] Machado, E. L., Dambros, V. S., Kist, L. T., Lobo, E. A. A., Tedesco, S. B., Moro, C. C. Use of Ozonization for the Treatment of Dye Wastewaters Containing Rhodamine B in the Agate Industry. *Water Air Soil Pollut*. 2012, 223, 1753-1764.
- [3] Schneider, I. A. H., Pizzolato, T. M., Machado, Ê. L., Carissimi, E. I-028 - Fotodegradação solar e oxidação química (NaOCl) de corantes empregados na indústria de tingimento de ágatas. XXVII Congresso Interamericano de Engenharia Sanitária e Ambiental. ABES - Associação Brasileira de Engenharia Sanitária e Ambiental. 2000.
- [4] Richardson, S. D., Wilson, C. S., Rusch, K. A. Use of rhodamine water tracer in the marshland upwelling system. *Ground Water*. 2004, 42-5, 678-688.
- [5] Jain, R., Mathur, M., Sikarwar, S., Mittal, A. Removal of the hazardous dye rhodamine B through photocatalytic and adsorption treatments. *J. of Environmental Management*. 2007, 85 (4), 956-964.
- [6] Hu-sheng Chen, Ph. D. Identification of Rhodamine 6g and Rhodamine B dyes present in ballpoint pen inks using high-performance liquid chromatography and UV-Vis spectrometry. *Forensic Science Journal*. 2007, 6-1, 21-37.
- [7] Kornbrust, D., Barfknecht, T. Testing Dyes in HPC/DR systems. *Environmental Mutagenesis*. 1985, 7, 101.
- [8] McGregor, D. B., Brown, A. G., Howgate, S., McBride, D., Riach, C., Caspary, W. J., Carver, J. H. Responses of the L5178Y mouse lymphoma cell forward mutation assay. V: 27 coded chemicals. *Environmental and Molecular Mutagenesis*. 1991, 17, 196.

- [9] Pizzolato, T. M., Carissimi, E., Machado, E. L., Schneider, I. A. H. Colour removal with NaClO of dye wastewater from an agate-processing plant in Rio Grande do Sul. *International Journal of Mineral Processing*. 2002, 65, 203-211.
- [10] Sivamani, S., Grace, B. L. Removal of Dyes from Wastewater using Adsorption - A Review. *International Journal of BioSciences and Technology*. 2009, 2-4, 47-51.
- [11] Grassi, M., Kaykioglu, G., Belgiorno, V., Lofrano, G. Removal of Emerging Contaminants from Water and Wastewater by Adsorption Process. G. Lofrano (ed.), *Emerging Compounds Removal from Wastewater*, Springer. *Briefs in Green Chemistry for Sustainability*. 2012, 15-35.
- [12] Fungaro, D. A., Yamaura, M., Carvalho, T. E. M., Graciano, J. E. A. Zeolite from Fly Ash-Iron Oxide Magnetic Nanocomposite: Synthesis and Application as an Adsorbent for Removal of Contaminants from Aqueous Solution. In: ANDREYEV, M. K; ZUBKOV, O. L. (Ed.). *Zeolites: Synthesis, Chemistry and Applications*. Hauppauge (pp. 93-122). N.Y.: Nova Science Publishers. 2012.
- [13] Fungaro, D. A., Izidoro, J. C., Santos, F. S., Wang, S. Coal Fly Ash from Brazilian Power Plants: Chemical and Physical Properties and Leaching Characteristics. In: SARKER, P.K. (Ed.). *Fly Ash: Chemical Composition, Sources and Potential Environmental Impacts* (pp. 145-164). Hauppauge, N.Y.: Nova Science Publishers. 2013.
- [14] Li, Z., Bowman, R. S. Counterion effects on the sorption of cationic surfactant and chromate on natural clinoptilolite. *Environmental Science & Technology*. 1997, 31, 2407-2412.
- [15] Bowman, R. S. Review: Applications of surfactant-modified zeolites to environmental remediation. *Microporous and Mesoporous Materials*. 2003, 61 (1), 43-56.
- [16] Echeverría, J. C., Zarranz, I., Estella, J., Garrido J. J. Simultaneous effect of pH, temperature, ionic strength, and initial concentration on the retention of lead on illite. *Applied Clay Science*. 2005, 30 (2), 103-115.
- [17] Ramakrishna, K.R., Viraraghavan, T. Dye removal using low cost adsorbents. *Water Sci. Technol*. 1997, 36, 189-195.
- [18] Ponnusami, V., Krithika, V., Madhuran, R., Srivastava, S. N. Biosorption of reactive dye using acid-treated rice husk: Factorial design analysis. *J. of Hazardous Materials*. 2007, 142, 397-403.
- [19] Cestari, A. R., Vieira, E. F. S., Mota, J. A. The removal of an anionic red dye from aqueous solutions using chitosan beads—The role of experimental factors on adsorption using a full factorial design. *Journal Hazardous Materials*. 2008, 160 (2-3), 337-343.
- [20] Fungaro, D. A., Borrely, S. I. Synthesis and characterization of zeolite from coal ashes modified by cationic surfactant. *Cerâmica*. 2012, 58 (345), 77-83.
- [21] Izidoro, J. C., Fungaro, D. A., Santos, F. S., Wang, S. Characteristics of Brazilian coal fly ashes and their synthesized zeolites. *Fuel Processing Technology*. 2012a, 97, 38-44.
- [22] Haggerty, G. M., Bowman R. S. (1994). Sorption of chromate and other inorganic anions by organo-zeolite. *Environmental Science & Technology*. 1994, 28 (3), 452-458.
- [23] Scott, J., Guang, D., Naeramitarnasuk, K., Thabuot, M., Amal, R. Zeolite synthesis from coal fly ash for the removal of lead ions from aqueous solution. *Journal of Chemical Technology and Biotechnology*. 2001, 77, 63-69.
- [24] Lagergren, S. On the theory of so-called adsorption dissolved substances. *Handlingar Band*. 1898, 24, 1-39.
- [25] Ho, Y. S., McKay, G. Comparative sorption kinetic studies of dye and aromatic compoundson to fly ash. *Journal of Environmental Science and Health*. 1999, A-34 (5), 1179-1204.
- [26] Foo, K. Y., Hameed, B. H. Insights into the modeling of adsorption isotherm systems. *Chemical Engineering Journal*. 2010, 156 (1), 2-10.
- [27] Ng, J. C. Y., Cheung, W. H., McKay, G. Equilibrium Studies of the Sorption of Cu (II) Ions onto Chitosan. *Journal of Colloid and Interface Science*. 2002, 255, 64-74.
- [28] Ho, Y. S. Selection of optimum sorption isotherm. *Carbon*. 2004, 42 (10), 2115-2116.
- [29] Ncibi, M. C., Mahjoub, B., Seften, M. Kinetic and equilibrium studies of methylene blue biosorption by *Posidonia oceanica* (L.) fibres. *Journal of Hazardous Materials*. 2007, B139, 280-285.
- [30] Murayama, N., Yamamoto, H., Shibata, J. Mechanism of zeolite synthesis from coal fly ash by alkali hydrothermal reaction. *International Journal of Mineral Processing*. 2002, 64, 1-17.
- [31] Tanaka, H., Sakai, Y., Hino, R. Formation of Na-A and -X zeolites from waste solutions in conversion of coal fly ash to zeolites. *Materials Research Bulletin*. 2002, 37, 1873-1884.
- [32] Pires, M., Querol, X. Characterization of Candiota (South Brazil) coal and combustion by-product. *International Journal of Coal Geology*. 2004, 60, 57-72.

- [33] Chao, H-P., Chen, S-H. Adsorption characteristics of both cationic and oxyanionic metal ions on hexadecyltrimethylammonium bromide-modified NaY zeolite. *Chemical Engineering Journal*. 2012, 193-194, 283-289.
- [34] Izidoro, J. C., Fungaro, D. A., Wang, S. Zeolite synthesis from Brazilian coal fly ash for removal of Zn²⁺ and Cd²⁺ from water. *Advanced Materials Research*. 2012b, 356-360, 1900-1908.
- [35] Hemmings, R. T., Berry, E. E. Speciation in Size and Density Fractionated Fly Ash. *MRS Proceedings*. 1985, 65, 91.
- [36] Umanã-Penã, J. C. Síntesis de zeólitas a partir de cenizas volantes de centrales termoeléctricas de carbón. Doctoral thesis. Universitat Politècnica de Catalunya, Espanha. 2002.
- [37] Nidheesh, P. V., Gandhimathi, R., Ramesh, S. T., Anantha Singh, T. S. Investigation of Equilibrium and Thermodynamic parameters of Crystal Violet Adsorption onto Bottom Ash. *Journal International Environmental Application & Science*. 2011, 6 (4), 461-470.
- [38] Nidheesh, P. V., Gandhimathi, R., Ramesh, S. T., Anantha Singh, T. S. Kinetic analysis of crystal violet adsorption on to bottom ash. *Turkish J. Engineering Environment Science*. 2012, 36, 249-262.
- [39] Jha, B., Singh, D. N. A Review on Synthesis, Characterization and Industrial Applications of Fly ash Zeolites. *Journal of Materials Education*. 2011, 33 (1-2), 65-132.
- [40] Paprocki, A. Síntese de zeólitas a partir de cinzas de carvão visando sua utilização na descontaminação de drenagem ácida de mina. Master's thesis. Porto Alegre, Brazil, Pontificia Universidade Católica do Rio Grande do Sul. 2009.
- [41] Sijakova-Ivanova, T., Panov, Z., Blazev, K., Zajkova-Paneva V. Investigation of fly ash heavy metals content and physicochemical properties from thermal power plant. *International Journal Engineering Science Technology*. 2011, 3(12), 8219-8225.
- [42] Mouhtar, T., Charistos, D., Kantiranis, N., Filippidis, A., Kassoli-Fournaraki, A., Tsirambidis, A. GIS-type zeolite synthesis from Greek lignite sulphate fly ashes promoted by NaOH solutions. *Microporous Mesoporous Materials*. 2003, 61, 57-67.
- [43] Lee, W. K. W., van Deventer, J. S. J. The effects of inorganic salt contamination on the strength and durability of geopolymers. *Colloids and Surfaces A: Physicochemical and Engineering Aspects*. 2002, 211, 115-126.
- [44] Chindaprasit, P., Jaturapitakkul, C., Chalee, W., Rattanasak, U. Comparative study on the characteristics of fly ash and bottom ash geopolymers. *Waste Management*. 2009, 29 (2), 539-543.
- [45] Covarrubias, C., García, R., Arriagada, R., Yáñez, J., Garland, M. T. Cr (III) exchange on zeolites obtained from kaolin and natural mordenite. *Microporous and Mesoporous Materials*. 2006, 88 (1-3), 220-231.
- [46] Bansiwala, A. K., Rayalu, S. S., Labhasetwar, N. K., Juwarkar, A. A., Devotta, S. Surfactant-modified zeolite as a slow release fertilizer for phosphorus. *Journal of Agricultural and Food Chemistry*. 2006, 54 (13), 4777-4779.
- [47] Giles, C. H., MacEwan, T. H., Nakhwa, S. N., Smith, D. Studies in Adsorption. Part XI. A System of Classification of Solution Adsorption Isotherms, and its Use in Diagnosis of Adsorption Mechanisms and in Measurement of Specific Surface Areas of Solids. London. 1960, 3973-3993.
- [48] Tempkin, M. J., Pyzhev, V. Recent modification to Langmuir isotherms, *Acta Physicochim. USSR*. 1940, 12, 217-222.
- [49] Liu, Y. Is the free energy change of adsorption correctly calculated. *Journal Chemical & Engineering Data*. 2009, 54, 1981-1985.
- [50] Lundstedt, T., Seifert, E., Abramo, L., Thelin, B., Nystrom, A., Pettersen, J., Bergman, R. Experimental design and optimization. *Chemometrics and Intelligent Laboratory Systems*. 1998, 42, 3-40.
- [51] Abdel-Ghani, N. T., Hefny, M. M., EL-Chaghaby, G. A. Removal of Metal Ions from Synthetic Wastewater by Adsorption onto Eucalyptus Camaldulensis Tree Leaves. *Journal of the Chilean Chemical Society*. 2008, 53 (3), 1585-1587.

Raquel R. Alcântara is Master's student in Chemistry and Environment at the Sao Paulo University, Sao Paulo, Brazil, Bachelor and degree in chemistry
E-mail address: rreisa@hotmail.com

Rafael O. R. Muniz is graduated in Physics at the Catholic Sao Paulo University and a masters in Nuclear Technology - Reactors at the Sao Paulo University and a PhD in Nuclear Technology - Reactors at the Sao Paulo University.
E-mail address: rafael.orm@gmail.com

Denise A. Fungaro is Ph.D. of Science in Chemistry from the Sao Paulo University, Sao Paulo, Brazil, Research on Synthesis and Characterization of low-cost Nanomaterial and its Application as Adsorbent for the Treatment of Wastewater.
E-mail address: dfungaro@ipen.br